Dalton Transactions

PAPER

View Article Online
View Journal | View Issue

Cite this: *Dalton Trans.*, 2014, **43**, 7269

Insights into the coordination mode of quercetin with the Al(III) ion from a combined experimental and theoretical study†

Emilia Furia,*[a] Tiziana Marino[a] and Nino Russo[a,b]

Received 21st January 2014,
Accepted 1st March 2014

DOI: 10.1039/c4dt00212a

www.rsc.org/dalton

Combining potentiometric, spectroscopic and theoretical DFT computations we have studied the formation of the Al(III)–quercetin complex in ethanol solution. The possible complexation sites have been considered on the basis of all the experimental and theoretical tools used. Results supported proposing a 1 : 1 neutral complex and the possibility to have different isomers in solution.

Introduction

Flavonoids, the most abundant polyphenolic natural antioxidant compounds, are found in most plants, concentrating in seeds, fruit skin or peel, bark and flowers, and in a variety of beverages (tea, coffee, wines and fruit drinks).[1] Flavonoids have been shown to have a variety of beneficial biological effects, including protection of cells against oxidative stress and antibacterial, anti-inflammatory and vasodilator activities.[2–4] Polyphenol-rich diets have been repeatedly correlated with a low risk of developing cardiovascular diseases and cancers, the two major causes of mortality in Western countries.[5]

Quercetin (3,3′,4′,5,7-pentahydroxyflavone, H_5Que), one of the most common flavonols present in nature (*i.e.* in grapes, onions, berries, green vegetables and legumes), has attracted the attention of many researchers due to its biological properties.[6–10] In addition, it is well known that quercetin may chelate metal ions, preventing the metal-mediated generation of damaging oxidizing radicals and protecting the biological targets against oxidative stress.[11–14] In the quercetin structure three chelation sites are possible: the 3-hydroxy-carbonyl, the 5-hydroxy-carbonyl and the 3′,4′-dihydroxyl functions (Scheme 1).[15,16]

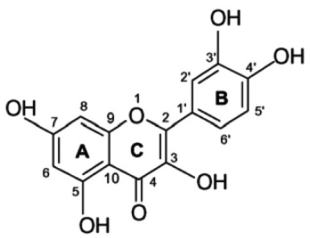

Scheme 1 Chemical structure of quercetin (H_5Que).

Previous experimental and theoretical investigations have focused on the complexation of Fe(II) and Fe(III),[17,18] Cu(II)[19] and Pb(II)[20] with quercetin in solution and at different stoichiometric ratios. The Al(III)–quercetin complex has been previously studied at theoretical and experimental levels in solid phase[21] and in solution by combining spectroscopic UV measurement and the semiempirical AM1 theoretical method.[22] Furthermore, two other joint experimental and density functional studies concern the complex in which the experimental conditions give a stoichiometric ratio of 1 : 2, metal : ligand.[23,24] Finally, the ability of flavonoids to form chelate complexes with a series of metals has recently been briefly reviewed.[25]

Despite the presence of these studies, the composition, structure and complex formation features are not exhaustively investigated and are sometimes contradictory.[17–21]

In this work, we have studied the complexation of quercetin with the Al(III) ion in solution by using a combination of experimental (potentiometric measurements and IR and UV spectra) and computational (density functional theory) tools in order to obtain the structural and electronic properties of the resulting complex.

Compared to previous work on this subject, we underline that in our investigation we use potentiometric and spectrophotometric measurements in a wide range of pH and

[a]*Dipartimento di Chimica e Tecnologie Chimiche, Università della Calabria, P Bucci, I-87036 Arcavacata di Rende, Italy. E-mail: emilia.furia@unical.it*
[b]*Departamento de Quimica, Division de Ciencias Basicas e Ingenieria, Universidad, Autonoma Metropolitana-Iztapalapa, Av. San Rafael Atlixco No. 186, Col. Vicentina, CP 09340 Mexico D.F., Mexico*

†Electronic supplementary information (ESI) available: The primary data comprise 4 titrations with 65 data points, and summary of the relevant data taken in all titrations have been reported in Table S1. The computed and experimental vibrational spectra of metallated complexes have been reported in Fig. S1 and S2, respectively. The distribution diagram of the Al(III) ion in the hydrolytical species has been reported in Fig. S3. See DOI: 10.1039/c4dt00212a

first principle computations in a molar complex ratio of 1 : 1 (metal : ligand), as indicated by the experimental data but scarcely investigated previously.

The reason for choosing the aluminium cation is mainly due to the fact that it is the third most abundant element in the Earth's crust and often enters the biotic cycle in many different ways.[26] The human exposure to aluminium was not fully explained but it is well known that it does not serve any essential function in human biochemistry.[26] By contrast, the Al(III) cation can enter the brain where it persists for a long time and a small increase seems sufficient to produce neurotoxicity.[27] For this reason, the presence of aluminium in the human brain has been associated with Alzheimer's and other neurodegenerative diseases.[28] Chelation therapy with some ligands has been demonstrated to reduce some of the aluminium toxicity.[26,28] In this context, it is interesting to explore the ability of a natural product such as quercetin to coordinate the Al(III) ion.

Experimental and theoretical details

Computational details

Full optimization in solution without any symmetry restriction has been carried out at the DFT level employing the M052x[29] exchange-correlation functional coupled with the 6-31+G(d) basis set for all atoms. Solvent effects have been described through a continuum approach by means of the SMD version of the polarizable continuum model (PCM).[30] The dielectric constant of ethanol has been fixed at 24.85. Vibrational frequencies have been computed on each optimized structure at the same level of theory of the optimizations, and zero point vibrational corrections have been added to the electronic energies. The TD-DFT approach[31] has been used to obtain the vertical excitation energies. In these computations different hybrid and meta-hybrid exchange-correlation functionals (M052x,[29] M06[32] and wB97XD[33]) have been employed.

All the computations have been performed using the Gaussian (G03) suite of programs.[34]

Potentiometric measurements

The perchloric acid stock solution and the sodium hydroxide titrant solutions have been prepared and standardized as previously described.[35,36] A sodium perchlorate stock solution has been prepared and standardized according to Biedermann.[37] Aluminium(III) perchlorate has been prepared and standardized as reported by Ciavatta and Iuliano.[38] All solutions have been prepared with ethanol. The cell arrangement was similar to that described by Forsling and Hietanen.[39] Ag/AgCl electrodes have been prepared according to Brown.[40] Glass electrodes, manufactured by Metrohm, have been of the 6.0133.100 type. They acquired, after the addition of the reagents, a constant potential within 15 min that remained unchanged within ±0.1 mV for several hours. The titrations have been carried out with a programmable computer controlled data acquisition switch unit 34970 A supplied by Hewlett Packard. The EMF values have been measured with a precision of $\pm 10^{-5}$ V using an OPA 111 low-noise precision DIFET operational amplifier. A slow stream of nitrogen gas has been passed through three bottles (a–c) containing: (a) 1 M NaOH, (b) 1 M H_2SO_4 and (c) 0.16 M $NaClO_4$, and then into the test solutions, stirred during titrations, through the gas inlet tube. During the EMF measurements, the cell assembly has been placed in a thermostat kept at 310.1 ± 0.1 K.

Vibrational spectra

The solid-state IR spectra (in KBr pellets) have been recorded on a Perkin-Elmer Spectrum One FT-IR spectrometer equipped for reflectance measurements.

Spectrophotometric measurements

The spectrophotometric measurements have been conducted with a Varian Cary 50 Scan UV visible spectrophotometer. Absorbance values between 250 and 550 nm have been measured at each 5 nm. The temperature of the cell holder has been kept at 310.1 ± 0.3 K by a Grant circulating water bath. Matched quartz cells of thickness 1 cm have been employed. The absorbance, A_λ, has been recorded to 0.001 units. The formulation of the parameters and the acquisition of the data have been managed with the aid of a computer connected to the tool.

Results and discussion

A sensitive tool to attain information on the formation and stoichiometry of metal complexes is potentiometric analysis. This methodology allows us to measure potential difference as a function of ion concentration in solution. The complex formation equilibria between Al(III) and quercetin has been studied using ethanol as a solvent at 310.15 K and in 0.16 M $NaClO_4$ by measuring with a glass electrode the competition of the ligand (H_5Que) for the aluminium(III) and H^+ ions. The metal (C_M) and ligand (C_L) concentrations ranged from 0.5 to 5 mM (the ligand-to-metal ratio varied between 1 and 10). The hydrogen ion concentration has been varied from 25 mM (pH 1.6) to incipient precipitation of basic salts which takes place in the range $[H^+]$ = 1.6–0.25 mM (pH 2.8–3.6) depending on the specific ligand-to-metal ratio. A summary of the relevant data taken in all titrations is reported in Table S1.† The general equilibrium can be written as follows:

$$p\mathrm{Al}^{3+} + r\mathrm{H_5Que} \rightleftarrows \mathrm{Al}_p\mathrm{H}_{-q}(\mathrm{H_5Que})_r^{(3p-q)} + q\mathrm{H}^+ \qquad \beta_{pqr}. \quad (1)$$

This formulation takes into account the possible formation of simple ($q = r$), mixed ($q \neq r$), mononuclear ($p = 1$) and polynuclear ($p > 1$) species. The most probable p, q and r values and the corresponding constants β_{pqr} have been obtained by least squares fitting of the potentiometric data.[41] In the numerical treatments the first three acidic constants of quercetin, according to equilibria (2)–(4) and reported with the relative standard deviation, have been kept invariant:

$$H_5Que \rightleftarrows H_4Que^- + H^+ \qquad \log K_{a1} = -8.40 \pm 0.01 \quad (2)$$

$$H_4Que^- \rightleftarrows H_3Que^{2-} + H^+ \qquad \log K_{a2} = -7.83 \pm 0.06 \quad (3)$$

$$H_3Que^{2-} \rightleftarrows H_2Que^{3-} + H^+ \qquad \log K_{a3} = -7.91 \pm 0.09 \quad (4)$$

These constants have been determined by potentiometric measurements under the same experimental conditions used for the stability constant evaluation between metal and ligand ions (*i.e.* in ethanol as a solvent at 310.15 K and in 0.16 M $NaClO_4$). The last two acidic constants of quercetin have not been considered due to the experimental pH range (*i.e.* 1.6–3.6).

The equilibrium constants for $AlOH^{2+}$, $Al(OH)_2^+$ and $Al(OH)_4^-$ have been kept fixed during the numerical treatment because they are well known from the literature.[42] Various models have been tested by adding a single species during the elaboration; the best agreement has been obtained with the neutral complex $Al(H)_{-3}(H_5Que)$, in which the metal–ligand stoichiometry is 1 : 1 and whose stability constant, $\log \beta_{1-31}$, is −5.79 ± 0.06 (the uncertainty represents 3σ) according to the general equilibrium (1). As no other species lowered the minimum, this model has been assumed to be the best data fitting, taking into consideration that the standard deviation (σ = 0.4) is comparable with the experimental uncertainty (σ = 0.2).

The refined equilibrium constant as previously determined has been used to represent the distribution of the metal in the different species (see Fig. 1).

As can be seen from Fig. 1, the proposed complex is formed in appreciable amounts and none of the hydrolytic species reach a significant percentage. Information regarding the structure and the coordination sites of the dissolved metal ion complex cannot be obtained using the employed experimental method but can be supplied by high level theoretical investigation.

Following indications from the potentiometric measurements, we have considered complexes with zero total charge and with the aluminium ion that retains the esa-coordination (see Scheme 2).

The considered complexes include structures in which quercetin is deprotonated in 3 or 5 positions and with the Al ion bi-coordinated with quercetin and surrounded by two water molecules and two OH groups (see a3-4 and a4-5 species in Scheme 2), or deprotonated in both 3 and 5 positions and

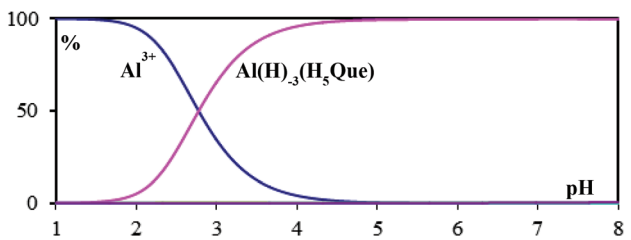

Fig. 1 Distribution of Al(III) species for C_L = 5 × 10^{-3} mol dm^{-3}, C_M = 5 × 10^{-3} mol dm^{-3}.

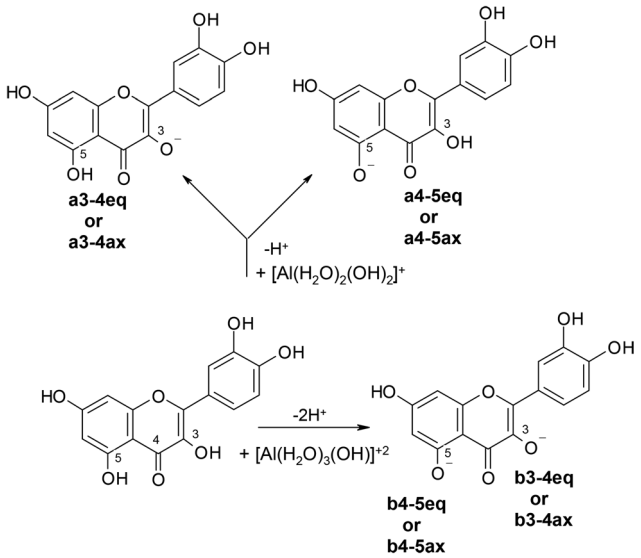

Scheme 2 Formation of the investigated Al-complexes starting from the considered deprotonated forms of quercetin.

linked to the $Al(H_2O)_3(OH)$ moiety (see b3-4 and b4-5 species in Scheme 2). The complex resulting from neutral ligand has not been considered, on the basis of the pH range of the experimental solutions. In all cases both the equatorial (**a3-4eq**, **a4-5eq** and **b4-5eq**, **b4-5eq**) and axial (**a3-4ax**, **a4-5ax** and **b4-5ax**, **b4-5ax**) topologies for the OH groups have been considered. The energetic data are collected in Table 1.

Results show that the complex in which the metal is coordinated to positions 4 and 5 between rings A and C (**a4-5ax**) is the most stable.

In the next lying minimum, at 2.9 kcal mol^{-1}, the Al ion coordinates to the C=O moieties in 3 and 4 positions inside ring C (**a3-4eq**). The zero charge complexes derived by deprotonation of both 3 and 5 O–H groups are higher in energy by 5.1 kcal mol^{-1} (**b3-4eq**) and 5.9 kcal mol^{-1} (**b4-5eq**), respectively (see Table 1). The structures of the two complexes have been reported in Fig. 2.

Greater stability is reached when a six membered ring is formed upon the coordination process. From the obtained

Table 1 Total (hartree) and relative (kcal mol^{-1}) energies for the neutral species

Species	E_{ZPE}	ΔE
$H_4QueAl(H_2O)_2(OH)_2$		
a3-4eq	−1650.390618	2.9
a3-4ax	−1650.389227	3.6
a4-5eq	−1650.393320	1.2
a4-5ax	−1650.395214	0.0
$H_3QueAl(H_2O)_3(OH)$		
b3-4eq	−1650.387088	5.1
b3-4ax	−1650.383435	7.4
b4-5eq	−1650.385786	5.9
b4-5ax	−1650.383394	7.4

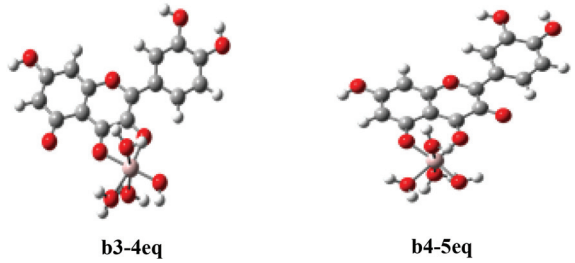

Fig. 2 M052x optimized structures of **b3-4eq** and **b4-5eq** complexes.

structures it emerges that the coordination occurs in a planar arrangement in all the studied species. In Table 2 are reported the geometrical parameters involving the coordination of a metal ion for all the optimized structures.

In the most stable structure (**a4-5ax**) the Al–O5 distance is 1.882 Å while the Al–O4 one is 1.952 Å reflecting the fact that the C–O5 bond is 1.309 Å *versus* the 1.273 Å of the C═O4 carbonyl bond. The behaviour in all other studied structures is similar. The O4–Al–O5 angle is 91° in **a4-5ax** while it assumes a smaller value when the coordination occurs with the oxygen atoms that lie in the same ring (*e.g.* 81.7° in **a3-4eq**). From the pH of the experimental solution and according to equilibria (3) and (4), we can reasonably hypothesize that both O3–H and O5–H groups, which have very similar pK_a (7.83 ± 0.06 and 7.91 ± 0.09), undergo deprotonation. In this context it is interesting to further consider the corresponding complexes **b3-4eq** and **b4-5eq** even if they exhibit a slightly reduced energetic stability. These two complexes differ in energy by only 0.8 kcal mol^{-1} and can be both populated under the experimental conditions. In order to have further insights into this possibility we have considered the interconversion process that can occur throughout the rotation of the $Al(H_2O)_3(OH)$ fragment around the C–O bond (Ψ angle in Fig. 3). Along this path we have located a transition state that lies at 5.8 kcal mol^{-1} above the lowest minimum (Fig. 3). This result suggests that interconversion between the **b3-4eq** and **b4-5eq** isomers is kinetically possible and both species should be present in solution.

The computed and experimental vibrational spectra of metallated complexes are reported in Fig. S1 and S2,† respectively, while the main stretching modes that can be affected by the complex formation are given in Table 3. We underline that the obtained experimental spectra concern the solid phase while the simulated ones refer to the liquid phase. Since our work is mainly devoted to the complexation process in solution we think that the comparisons can be regarded with caution.

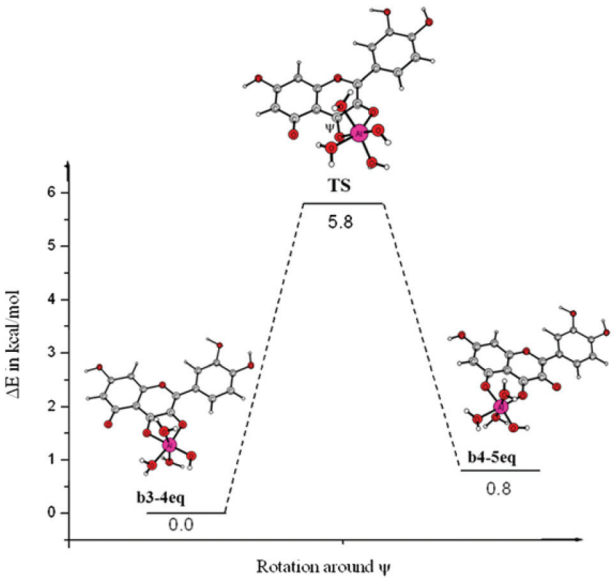

Fig. 3 Potential energy profile for the interconversion process as a function of the rotation around the C–O bond (Ψ angle) between **b3-4eq** and **b4-5eq** isomers.

Table 3 Selected calculated and experimental vibrational frequencies (cm^{-1}) of the Al(III)–quercetin complex

Mode	b3-4eq	b4-5eq
C_3–O_3	1634	1576
C_4–O_4	1582	1540
C_5–O_5	1390	1371
Exp	1638, 1596, 1579, 1545, 1514, 1374, 1328	

Table 2 Main geometrical parameters of the investigated structures by using two different protonation states of quercetin. Distances are in Å and angles are in degrees (°)

	$H_4QueAl(H_2O)_2(OH)_2$						
Species	Al–O3	Al–O4	Al–O5	Al–Ow	Al–OH	O3–Al–O4	O4–Al–O5
a3-4eq	1.896	1.982	—	2.045	1.811	81.7	—
a3-4ax	1.902	1.957	—	1.999	1.836	83.3	—
a4-5eq	—	1.957	1.891	2.026	1.820	—	88.5
a4-5ax	—	1.952	1.882	1.998	1.827	—	91.0
	$H_3QueAl(H_2O)_3(OH)$						
b3-4eq	1.857	1.910	—	1.987	1.787	84.4	—
b3-4ax	1.860	1.903	—	1.966	1.797	85.2	—
b4-5eq	—	1.865	1.848	1.987	1.799	—	93.2
b4-5ax	—	1.868	1.838	1.982	1.801	—	93.8

Table 3 clearly shows that the considered C–O vibrational modes in the **b4-5eq** assume values lower than that in the corresponding **b3-4eq** complex. Looking at the experimental values in the frequency range that includes the C–O vibrational modes we note that the 1579, 1545 and 1374 cm^{-1} fit well with the three C–O stretchings computed for the **b4-5eq** structure.

To gain additional insight into the complex formation, we have compared the UV-vis spectra of free and bound quercetin. The absorption spectrum of quercetin 0.1 mM in ethanol solution is presented in Fig. 4 (line 1).

Quercetin exhibits a strong absorption band at 368 nm. Upon addition of $Al(ClO_4)_3$ to quercetin in solution (1 : 1 ratio of Al(III) salt : H_5Que) the UV-vis data showed a 60 nm bathochromic (red) shift in absorbance (of the corresponding peak for quercetin) indicating that complexation occurs (Fig. 4, line 2). Moreover an isosbestic point has been observed at 392 nm, confirming the presence of the two species in equilibrium and therefore the formation of the complex.

In order to obtain further information on the origin of the UV-vis spectra we have computed the excitation energies for quercetin and two more probable complexes (**a3-4eq** and **b4-5eq**) by using different exchange-correlation functionals in the framework of time-dependent density functional theory.[31] Results are reported in Table 4.

For quercetin, although all the employed exchange-correlation functionals reproduce well the experimental data, better agreement has been found in the M06 values. For this system, the main bands at 255 and 368 nm are due to a HOMO → LUMO+1 (42%) and a HOMO → LUMO (69%) orbital transition, respectively. In the **a3-4eq** and **b4-5eq** species, the two main transitions have originated from the HOMO−4 → LUMO (about 70%) and HOMO → LUMO (about 60%) excitations. The M06 excitation energies for the considered complexes give results closer to the experimental absorption for the **a3-4eq** species, while the other two functionals seem to privilege the agreement with the **b4-5eq** complex. In any case the differences between the experimental and theoretical absorption spectra support the possibility that both the **a3-4eq** and **b4-5eq** isomers can contribute to the experimental UV-vis spectrum.

Since the presence of the complex (see Fig. 1) at physiological pH and the presence of $Al(OH)_4^-$ hydrolytical species in the absence of the ligand (see Fig. S3†) indicate that the ligand is able to quantitatively sequester the metal, our results can be related to the aluminium toxicity in living organisms since they highlight the properties and the formation process of the Al(III)–quercetin complex that can bind to the DNA affecting its transcription and, consequently, inhibit the growth of cancer cells.[25] In addition, our results can also be related to the reduction of toxic metal bioavailability, since the formation of the Al(III)–quercetin complex reduces excess aluminium in the diet thereby reducing the role of aluminium in neurological disorders.[20,21,25]

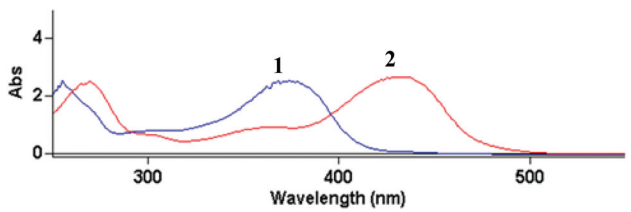

Fig. 4 UV-vis spectra of quercetin 0.1 mM (line 1) and of the complex formed between quercetin and $Al(ClO_4)_3$ 0.1 mM (line 2).

Table 4 Excitation energies (nm) and oscillator strength in parentheses for **a3-4eq**, **b4-5eq** and quercetin in ethanol computed by using different exchange-correlation functionals

a3-4eq	**b4-5eq**	Quercetin
M052x		
396 (0.50)	416 (0.63)	312 (0.59)
245 (0.54)	251 (0.48)	232 (0.49)
M06		
438 (0.37)	460 (0.55)	350 (0.48)
270 (0.37)	261 (0.24)	258 (0.21)
wB97XD		
400 (0.50)	426 (0.58)	317 (0.56)
247 (0.59)	251 (0.32)	234 (0.51)
Exp		
429, 269	429, 269	368, 255

Conclusions

In this work we have investigated the formation of the Al(III)–quercetin complex in solution by using a combination of experimental (potentiometric measurements, IR and UV spectra) and computational (density functional theory and time-dependent density functional theory) tools. From our results the following conclusions can be drawn:

– in the considered pH range, only complexes with a 1 : 1 stoichiometric ratio between metal and ligand are possible;

– the best fit of the potentiometric data indicates that the formed species should be neutral;

– DFT computations on the possible hydrated complexes indicate that the preferred complexation site of quercetin should be the deprotonated 3 and 5 positions of the A and C rings, respectively. Moreover, the transition between **a4-5ax** and **a3-4eq** requires a low barrier indicating that both species can be present in solution;

– the UV-vis experimental and theoretical spectra indicate possible coexistence of the two isomers in the ethanol solution;

– at physiological pH, quercetin is able to efficiently sequestrate the aluminium ion.

Acknowledgements

We gratefully acknowledge the Dipartimento di Chimica e Tecnologie Chimiche, Università della Calabria and PON R&C

(Programma Operativo Nazionale Ricerca e Competitività 2007–2013) project PON01_00293 "Spread Bio Oil" for financial support. N.R. thanks UAM for Càtedra Dr Raùl Remigio Cetina Rosado.

Notes and references

1 K. Herrmann, *J. Food Technol.*, 1976, **11**, 433.
2 C. L. M. Chantal, V. M. France, T. Muriel, S. M. Helene, M. Jacques and S. W. Marc, *Toxicology*, 1996, **114**, 19.
3 P. C. H. Hollman and M. B. Katan, *Food Chem. Toxicol.*, 1999, **37**, 937.
4 C. Polissero, M. J. P. Lenczowski, D. Chinzl, C. B. Davail, J. P. Sumpter and A. Fostier, *J. Steroid Biochem. Mol. Biol.*, 1996, **57**, 215.
5 B. Alluis and O. Dangles, *Helv. Chim. Acta*, 2001, **84**, 1133.
6 T. Leighton, C. Ginther, L. Fluss, W. Harter, J. Cansado and V. Notario, in *Phenolic Compounds in Foods and their Effects on Health II*, ed. T. Huang, C. T. Ho and C. Y. Lee, ACS Symposium Series 507, American Chemical Society, Washington, DC, 1992, p. 220.
7 P. Hollman, M. Hertog and M. Katan, *Food Chem.*, 1996, **57**, 43.
8 A. J. Moreira, C. Fraga, M. Alonso, P. S. Collado, C. Zetller, C. Marroni, N. Marroni and J. González-Gallego, *Biochem. Pharmacol.*, 2004, **68**, 1939.
9 M. Leopoldini, T. Marino, N. Russo and M. Toscano, *Theor. Chem. Acc.*, 2004, **111**, 210.
10 M. Leopoldini, T. Marino, N. Russo and M. Toscano, *J. Phys. Chem. A*, 2004, **108**(22), 4916.
11 I. B. Afanas'ev, A. I. Dorozhko, A. V. Brodskii, V. A. Kostyuk and A. I. Potapovitch, *Biochem. Pharmacol.*, 1989, **38**, 1763.
12 M. Melidou, K. Riganakos and D. Galaris, *Free Radical Biol. Med.*, 2005, **39**, 1591.
13 B. A. Halliwell and M. C. Gutteridge, *Biochem. J.*, 1984, **219**, 1.
14 G. Minotti and S. D. Aust, *Chem.-Biol. Interact.*, 1989, **71**, 1.
15 J. E. N. Dolatabadi, *Int. J. Biol. Macromol.*, 2011, **48**, 227.
16 M. Leopoldini, N. Russo and M. Toscano, *J. Agric. Food Chem.*, 2006, **54**, 3078.
17 A. Torreggiani, M. Tamba, A. Trinchero and S. Bonora, *J. Mol. Struct.*, 2005, **744**, 759.
18 M. Leopoldini, N. Russo, S. Chiodo and M. Toscano, *J. Agric. Food Chem.*, 2006, **54**, 6343.
19 J. Ren, S. Meng, C. E. Lekka and E. Kaxiras, *J. Phys. Chem. B*, 2008, **112**, 1845.
20 J. P. Cornard, L. Dangleterre and C. Lapouge, *J. Phys. Chem. A*, 2005, **109**, 10044.
21 A. Ahmedova, K. Paradoska and I. Wawer, *J. Inorg. Biochem.*, 2012, **110**, 27.
22 J. P. Cornard and J. C. Merlin, *J. Inorg. Biochem.*, 2002, **92**, 19.
23 L. Dangleterre, J. P. Cornard and C. Lapouge, *Polyhedron*, 2008, **27**, 1581.
24 Y. A. Davila, M. I. Sancho, M. C. Almandoz and S. E. Blanco, *Spectrochim. Acta, Part A*, 2012, **95**, 1.
25 M. Symonowicz and M. Kolanek, *Biotechnol. Food Sci.*, 2012, **76**(1), 35.
26 C. Exley, *Environ. Sci.: Processes Impacts*, 2013, **15**, 1807.
27 R. A. Yokel, *Curr. Inorg. Chem.*, 2012, **2**, 54.
28 C. Exley, *J. Inorg. Biochem.*, 1999, **76**, 133.
29 Y. Zhao, N. E. Schultz and D. G. Truhlar, *J. Chem. Theory Comput.*, 2006, **2**, 364.
30 A. V. Marenich, C. J. Cramer and D. G. Truhlar, *J. Phys. Chem. B*, 2009, **113**, 6378.
31 M. E. Casida, in *Recent Advances in Density Functional Methods, Part I*, ed. D. P. Chong, World Scientific, Singapore, 1995.
32 Y. Zhao and D. G. Truhlar, *Theor. Chem. Acc.*, 2008, **120**, 215.
33 J.-D. Chai and M. Head-Gordon, *Phys. Chem. Chem. Phys.*, 2008, **10**, 6615; J. D. Chai and M. Head-Gordon, *J. Chem. Phys.*, 2008, **128**, 84106.
34 M. J. Frisch, G. W. Trucks, H. B. Schlegel, G. E. Scuseria, M. A. Robb, J. R. Cheeseman, J. A. Montgomery Jr., T. Vreven, K. N. Kudin, J. C. Burant, J. M. Millam, S. S. Iyengar, J. Tomasi, V. Barone, B. Mennucci, M. Cossi, G. Scalmani, N. Rega, G. A. Petersson, H. Nakatsuji, M. Hada, M. Ehara, K. Toyota, R. Fukuda, J. Hasegawa, M. Ishida, T. Nakajima, Y. Honda, O. Kitao, H. Nakai, M. Klene, X. Li, J. E. Knox, H. P. Hratchian, J. B. Cross, C. Adamo, J. Jaramillo, R. Gomperts, R. E. Stratmann, O. Yazyev, A. J. Austin, R. Cammi, C. Pomelli, J. W. Ochterski, P. Y. Ayala, K. Morokuma, G. A. Voth, P. Salvador, J. J. Dannenberg, V. G. Zakrzewski, S. Dapprich, A. D. Daniels, M. C. Strain, O. Farkas, D. K. Malick, A. D. Rabuck, K. Raghavachari, J. B. Foresman, J. V. Ortiz, Q. Cui, A. G. Baboul, S. Clifford, J. Cioslowski, B. B. Stefanov, G. Liu, A. Liashenko, P. Piskorz, I. Komaromi, R. L. Martin, D. J. Fox, T. Keith, M. A. Al-Laham, C. Y. Peng, A. Nanayakkara, M. Challacombe, P. M. W. Gill, B. Johnson, W. Chen, M. W. Wong, C. Gonzalez and J. A. Pople, *Gaussian 03, Revision A.1*, Gaussian Inc., Pittsburgh, PA, 2003.
35 E. Furia and G. Sindona, *J. Chem. Eng. Data*, 2012, **57**, 195.
36 E. Furia, D. Aiello, L. Di Donna, F. Mazzotti, A. Tagarelli, H. Thangavel, A. Napoli and G. Sindona, *Dalton Trans.*, 2014, **43**, 1055.
37 G. Biedermann, *Sven. Kem. Tidskr.*, 1964, **76**, 362.
38 L. Ciavatta and M. Iuliano, *Ann. Chim.*, 1996, **86**, 1.
39 W. Forsling and S. Hietanen, *Acta Chem. Scand.*, 1952, **6**, 901.
40 A. S. Brown, *J. Am. Chem. Soc.*, 1934, **56**, 646.
41 P. Gans, A. Sabatini and A. Vacca, *J. Chem. Soc., Dalton Trans.*, 1985, 1195.
42 E. Furia and G. Sindona, *J. Chem. Eng. Data*, 2010, **55**, 2985.

